



A glimpse into the northernmost thermo-erosion gullies in Svalbard archipelago and their implications for Arctic cultural heritage

Ionut Cristi Nicu^{a,*}, Hakan Tanyas^b, Lena Rubensdotter^{c,d}, Luigi Lombardo^b

^a High North Department, Norwegian Institute for Cultural Heritage Research (NIKU), Fram Centre, N-9296 Tromsø, Norway

^b Faculty of Geo-Information Science and Earth Observation (ITC), University of Twente, PO Box 217, Enschede, AE 7500, Netherlands

^c Geological Survey of Norway (NGU), P.O. Box 6315 Torgarden, 7491 Trondheim, Norway

^d Arctic Geology Department, The University Centre in Svalbard (UNIS), P.O. Box 156, 9171 Longyearbyen, Norway

ARTICLE INFO

Keywords:

Thermo-erosion gullying

Thermokarst

Arctic

Svalbard

Cultural heritage

Climate change

ABSTRACT

Gully erosion is one of the most destructive geomorphological processes on relatively flat surfaces. This is exacerbated in the Arctic regions, where gullies are referred to as thermo-erosion gullies because of their unique connection to permafrost. As the surface of the permafrost freezes and thaws, soil particles destabilize, inducing erosion along preferential incisions, giving rise to widespread thermo-erosion gullies. In this study, we present the first thermo-erosion gully inventory in the Svalbard region (Nordenskiöld Land). The inventory was created using a combination of available aerial photographs from 2009 to 2011, direct field observations and measurements. The spatial distribution of thermo-erosion gullies is then exploited to investigate potential threats to the Arctic cultural heritage (CH). Analyses of thermo-erosion gullies are increasingly important for arctic administrations, which require more detailed hazard assessments as the effect of climate change becomes increasingly evident across these landscapes. The inventory is comprised of 810 thermo-erosion gullies in Nordenskiöld Land, most of which are located in close proximity to coastlines. We assess the inventory size statistics and correlation with terrain characteristics to investigate potential predisposing factors. No gullies occur at elevations greater than 200 m a.s.l., but gullies occur up to a maximum steepness of 37 degrees and along the whole topographic profile and, looking at the potential threat to CH, we found 44 of these sites within a 100 m buffer from the gullies. This distance is the reference that local administrations use to prioritize actions and safeguard the existence of arctic CH sites. In fact, a 100 m distance implies that future evolution of thermo-erosion gullies, especially enhanced by climate change may eventually erode away soil from the CH surroundings, threatening their stability and existence.

1. Introduction

Soil erosion has been internationally recognised as the most important process of land degradation (Montanarella and Panagos, 2021; Vanmaercke et al., 2021). Different processes of soil erosion are represented by sheet, rill, and gully erosion (Borrelli et al., 2017). Gully erosion, due to its various controlling factors, represents a very complex phenomenon that is present in all climatic areas worldwide: arid (Gurbanov and Ganieva, 2017) and semi-arid (Azareh et al. 2019), temperate-continental (Li et al. 2020; Nicu, 2021), continental (Li et al., 2016), sub-tropical (Luffman and Nandi, 2019), tropical (Sidle et al., 2019), Mediterranean (Martins et al., 2020), alpine (2017; Chen et al., 2018). Gully erosion has also been acknowledged in the Arctic (Godin

et al., 2019; Sidorchuk, 2020) and Antarctica (Gales et al., 2013; Dickson et al., 2017), as a result of global climatic changes on permafrost.

Permafrost is ground that has remained at or below 0 degreesC for two or more consecutive years (Schuur et al. 2015). The seasonal temperature fluctuations only induce thaw of the uppermost soil-layer, called the active layer, while the underlying soils and bedrock remain frozen. The current rapidly warming climate induces increasingly thicker active layers, as well as an increase in the temperature of the underlying permafrost, which, if passing 0 degreesC, is no longer permanently frozen (Obu et al., 2019). Within the Arctic and sub-Arctic areas, gullies are known as thermo-erosion gullies. A thermo-erosion gully may initiate when heat transfer from small water tracks penetrating the surrounding soils and increasing the depth of the active layer

* Corresponding author.

E-mail address: ionut.cristi.nicu@niku.no (I.C. Nicu).

<https://doi.org/10.1016/j.catena.2022.106105>

Received 6 November 2021; Received in revised form 28 December 2021; Accepted 1 February 2022

Available online 14 February 2022

0341-8162/© 2022 The Authors. Published by Elsevier B.V. This is an open access article under the CC BY license (<http://creativecommons.org/licenses/by/4.0/>).

locally. Below the active layer the ground remains permanently frozen with normally a very high ice content (up to over 90% in some circumstances but often around 75%) in the upper part of the permanently frozen part, called the *transition zone* (Iwahana et al., 2014). This ice-rich transition zone will, if thawed, release such excess of water that it may initiate both small scale fluvial processes and small slumps or grain collapses, if occurring in any kind of slope. Warmer or longer melting seasons may cause increasingly deeper active layers, thawing the ice-rich transition layer sediments and causing oversaturated soils. If the surface soils are removed by small scale gullying and/or slumping, new ice-rich soils will be exposed to thawing, initiating a feed-back loop of seasonal gully expansion. The geomorphological process may thus start humbly, for example during an unusual warm spell or prolonged thawing season one year, but as soon as a depression is formed, more gravitational slumping may accelerate the process rapidly. This, together with mechanical erosion and gravitational processes causes general soil subsidence and channel incision through thermo-erosion processes and results in a mixing of soil horizons and continued erosion of adjacent soils (Kokelj and Jorgenson, 2013). Thermo-erosion gullies enlarge both retrogressively upslope and through deepening and widening of the initial incision.

The rapidly increasing trend in temperature and precipitations since the 1970 s has initiated general permafrost degradation in many Arctic regions (Biskaborn et al., 2019), and has strong influences on landforms, ecosystems, geomorphological processes (Berthling et al., 2020), infrastructure (Hjort et al., 2018; Karjalainen et al., 2019), and society (Ford et al., 2021). The warming trend in the Arctic has been twice as rapid as the global average (Bintanja, 2018) and leads to increased and varied thermokarst activity: thawing ice-wedges, degrading pingos, thaw slumps, thermo-erosion gullies, coastal erosion, etc. These processes are also known as cryospheric hazards, which may pose a danger for both society (Ding et al., 2021) and cultural heritage (Ljungqvist et al., 2020). Svalbard is experiencing amplified climate change when compared to the global average (van Pelt et al., 2019), and represents a hot-spot for scientists to focus on: land cover and ice-wedge mapping (Bartsch et al., 2016; Lousada et al., 2018), the surface morphology of fans (De Haas et al., 2015), modelling the velocity of glaciers and ice caps (Strozzi et al., 2017), plastic pollution (Collard et al., 2021), glacier retreat (Kociuba et al., 2021) and coastal erosion (Jaskólski et al., 2018; Zagórski et al., 2020; Nicu et al., 2020; Nicu et al., 2021a).

With a scenario of continued increase in greenhouse gas emissions, climate change impacts for Arctic Norway and Svalbard towards the year 2100 is predicted to result in significant increase of mean annual air temperature (MAAT) and precipitation, and general decrease of snow, glaciers, sea ice, and permafrost across the whole latitude spectrum (Hanssen-Bauer et al., 2017). A few studies have approached thermo-erosion gullying in cold regions: Nunavut – Canada (Fortier et al., 2007; Godin and Fortier, 2012; Godin et al., 2014; Perreault et al., 2016, 2017), Alaska – USA (Tape et al., 2011; Lara et al., 2019), Yamal Peninsula – Russia (Sidorchuk and Matveeva, 2020; Sidorchuk, 2020), Greenland (Pastor et al., 2020; Christensen et al., 2021). Thermo-erosion gullies are of additional interest because through their evolution, they contribute to the release of vast amounts of methane (CH₄, a greenhouse gas), stored in the active layer. Therefore, studying thermo-erosion gullying also represents a base to identify source areas where a higher level of methane is being released into the atmosphere (Oberle et al., 2019). With all the efforts being made by scientists, the Arctic region of Svalbard has been ignored in regard to the thermo-erosion gullying process.

The general effects of climate change on global cultural heritages have been acknowledged and many studies tackled this issue (Sesana et al., 2021). While there are previous studies of gully erosion effects on cultural heritage at a global level (Nicu, 2018; Ciampalini et al., 2019; Nicu, 2019; Lombardo et al., 2020), there are no studies that approach the effects of thermo-erosion gullying on Arctic cultural heritage; even though about 180.000 archaeological sites are registered in the Arctic

(Hollesen et al., 2018). Climate change-induced processes affecting cultural heritage (Ford et al., 2006) is even less studied in Svalbard; with the only studies being very recent on thaw slumping (climate-induced landslides; see Nicu et al., 2021b), coastal erosion (Nicu et al. 2020; 2021a) and the decay of wooden features (Mattson et al., 2010, Flyen et al., 2020). In contrast, anthropogenic influence on cultural heritage in Svalbard, such as the Arctic tourism, has been studied in more detail (Hagen et al., 2012; Thuestad et al., 2015; Jaskólski, 2021).

The present study aims to i) create an inventory and have a general overview of thermo-erosion gullying in Nordenskiöld Land (Svalbard); ii) identify the main controlling factors of thermo-erosion gullying; iii) present the monitoring results of small-scale fluvial gullying; iv) analyse the implications of thermo-erosion gullying processes in regard to Arctic cultural heritage sites and a warming climate. All the above points will tackle the mentioned issues for the first time. The results of this study will shed light on the environmental factors controlling thermo-erosion gullying and may be used to evaluate the present state of cultural heritage sites as well as cultural heritage assessment and management. Local authorities and stakeholders in Svalbard are the main end-users of the results and will benefit in prioritising any future mitigation measures in the fast-changing Arctic landscape. Also, this contribution provides the first inventory of thermo-erosion gullying, creating the potential to monitor future development and speed of change, which is of interest not only for Arctic cultural heritage preservation, but for permafrost geomorphology and Arctic climate change in general. Moreover, knowledge of the factors controlling thermo-erosion gullying and their interactions is highly significant for developing effective gully management strategies.

2. Study area and Arctic cultural heritage

2.1. Study area

The study area is located in central Spitsbergen (Fig. 1), which is the largest island of the Svalbard archipelago (governed by Norway and established by the Spitsbergen Treaty from 9 February 1920); Svalbard archipelago, with an area of approximately 61020 km² is located ~ 1100 km south of the North Pole and ~ 800 km north of the coast of Norway (Zwoliński et al., 2013).

As a consequence of its location, Svalbard forms one of the most important and strategic terrestrial nodes on Earth, separating the Greenland Sea, the Barents Sea, and the Arctic Ocean (Jaskólski et al., 2018). Svalbard also represents one of the most diverse geological features in the world, where sections representing most of the Earth's history are accessible. Another significant characteristic of Svalbard's geology is the presence of terrestrially exposed sedimentary successions that are rare or do not exist in other places in northern Europe (Elvevold et al., 2007).

Nordenskiöld Land, named after the Finnish-Swedish geologist Nils Adolf Erik Nordenskiöld (Norwegian Polar Institute, 2021a,b), forms the largely ice-free peninsula between Van Mijenfjorden, Isfjorden and Bellsund. Geologically, the peninsula is part of the contact zone of two large structures of the first order: the horst-anticlinorium of the western coast of Spitsbergen and the West Spitsbergen graben like trough. Quaternary deposits are represented by raised marine sediments in the lowlands, glacial and glacio-fluvial deposits, extensive and complex slope deposits, areas of aeolian sediment cover and extensive in situ weathering of bedrock. The landscapes are diverse: from watershed peaks to the landscapes of U-shaped valleys, small valley glaciers and moraines, and coastal plains; peaks, mountains slopes, and moraines are covered by primary and desert-arctic soils with thin herbaceous-moss-lichen groups (Demidov et al., 2020). Both sediments and bedrock is influenced by the perennial frost in the ground (permafrost).

The climate of the area is influenced by the warm West Spitsbergen Sea Current and warm and humid air masses from the Atlantic Ocean; as a consequence, the air temperature is higher than would be expected for

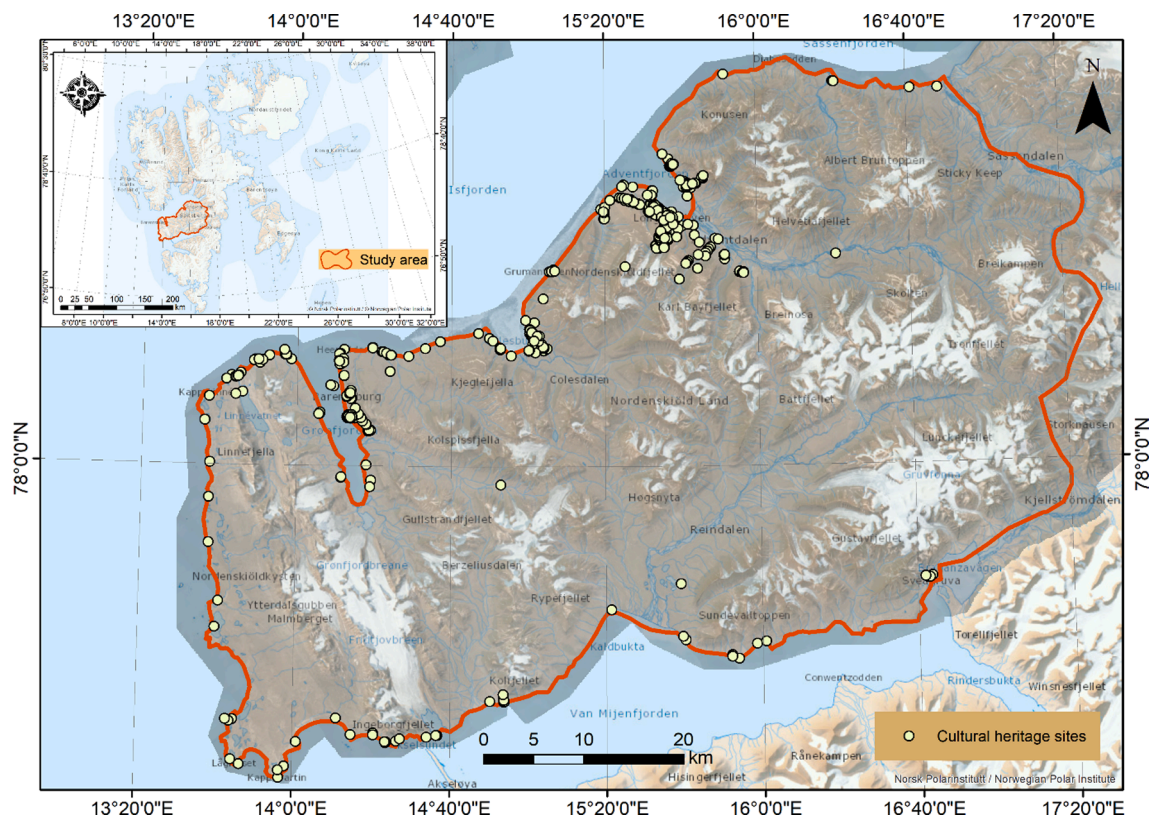


Fig. 1. General geographical location of Svalbard with detail over the Nordenskiöld Land area (including cultural heritage sites as points).

the Arctic latitude. There has been a considerable increase in the amount of precipitation over the last century; annual precipitation in 1940 was 482 mm and in 2018 was 704 mm. The highest amount of precipitation occurs from October to March (which overlaps with the period of high cyclonic activity), whilst the lowest amount occurs from April to July. Precipitation during the winter is 1.5–2 times higher compared to summer (Demidov et al., 2020). Also, the mean air temperature has increased over Svalbard by 3–5 degreesC between 1971 and 2017, with the greatest change in the winter months (Hanssen-Bauer et al., 2019).

From a hydrological point of view, the largest rivers in Nordenskiöld Land (greater than 20 km in length) are Coles, Gren, and Hollendar with an annual discharge of about 40 mil. m³. The continuous discharge of rivers lasts about 5 months, and it usually ends by the beginning of October (Romashova et al., 2019).

2.2. Arctic cultural heritage

Arctic cultural heritage represents a special type of heritage that needs extra attention and constant protection (Bogolyubova et al., 2019) due to the harsh conditions that are changing every year in a continuously warming climate. The Svalbard Environmental Protection Act states that all remains from before 1946 are automatically protected and considered cultural heritage sites, along with a 100 m buffer area around them. Cultural heritage in Svalbard is dominated by fragile wooden structures (Fig. 2a), and thermokarst (ground surface displacement and erosion caused by permanent degradation of permafrost) and solifluction (slow movement of surface soil on slopes caused by freeze and thaw processes) processes are therefore a real threat.

The threatened CH includes all types of constructions, like buildings (Fig. 2a) and remnants of houses (Fig. 2b), trapping devices and installations, from whaling, hunting, trapping (Fig. 2c), mining (Fig. 2d), scientific exploration up to and including World War II, grave markers (Fig. 2e), bones and bone fragments (Fig. 2f) (Governor of Svalbard). Out of these, graves are the most common cultural heritage sites in

Svalbard (Prestvold, 2008). There are about 8300 cultural heritage items officially registered in Svalbard and Nordenskiöld Land area holds about 10% of them (872 items, Fig. 1).

One of the first initiatives for the protection of Arctic cultural heritage was taken through the initiation of the Nordic Action Plan to Protect the Natural and Cultural Heritage of Arctic – Greenland, Iceland and Svalbard; the plan was aimed at contributing to the realisation of the goals in the Nordic Environmental Strategy and the Arctic Programme for Co-operation. It was approved on August 23, 1999, by the Nordic Environmental Ministers in Iceland (Nielsen, 2006).

Cultural heritage sites in the Arctic express the capability of the people to adapt to the cold climate and survive in tough conditions. Svalbard's cultural heritage has an even greater value when it is regarded as part of unique Svalbard's "haunted landscape" (Kinossian, 2020) and is considered to be internationally valuable (Hacquebord, 2001). Thus, monitoring and maintenance of cultural heritage sites in the Arctic is considered highly relevant (Dahle et al., 2000).

3. Methodology

In order to build a comprehensive thermo-erosion gully inventory for the study area, the most recent orthophotos (5 × 5 m pixel size) acquired in 2009–2011 from the Web Map Services (WMS) of the NPI (Norwegian Polar Institute/USGS Landsat, 2021) were interpreted. The gullies were identified morphologically and digitised on-screen as polygons and integrated into a GIS database. The data is stored in WGS_1984_UTM_Zone_33N coordinate reference system. Different parameters and statistical analyses were applied to understand the most important factors controlling thermo-erosion gullying.

To quantify the spatial distribution of gullies, we generated the point and area densities of gullies (i.e., the magnitude of number and size of gullies per unit area) using a Kernel Density function. To further analyse the size distribution of gullies, we also examined their frequency-area distribution (FAD). This procedure is particularly common in case of



Fig. 2. Examples of different cultural heritage features on Svalbard; a. Wooden Central cable-car in Hiorthhamn used for coal loading; b. Drone photo of trapping house remains located at Russekeila; c. Remains of trapping device in the proximity of Russekeila; d. Structural Remains of past mining activity near Svea; e. Restored Russian cross and grave at Russekeila; f. Whale skull remains on the shores between Russekeila and Isfjord Radio.

landslides, being used to identify the probabilities of landslides belonging to specific size bins. Specifically, the FAD of medium and large landslides has been long recognized as distribution exhibiting power-law scaling and the variation between the probabilities of different size bins characterized by the slope of the distribution, called power-law exponent (β ; e.g., Malamud et al., 2014). Topography is most likely the main factor controlling the β and thus, specific β ranges are often used in the literature for different environmental settings (e.g., ten Brink et al., 2009, Liucci et al., 2017). In this regard, FADs of landslides are exploited for various purposes including quantitative landslides hazard assessments (Guzzetti et al., 2005) or denudation caused by landslides (Hovius et al., 1997). However, size statistics of gullies has still not become commonplace in the context of gullies, although it could be potentially used to leverage our understanding regarding hazard caused by gully erosion. In this study, to identify β and the power-law fit for the FAD of our gully inventory, we used the code provided by Tanyas et al. (2018) and Clauset et al. (2009), respectively.

In addition to this, we also explored whether locations where gullies are present behave differently from locations where these processes are absent, in terms of terrain properties. Similarly, we assessed whether gullies have diagnostic morphological characteristics that can be retrieved from the polygonal inventory. We also analyse whether gullies originate in specific lithotypes. Lithotypes were extracted from the

Norwegian Polar Institute WebGIS service Geological Map, scale 1:250000 (Norwegian Polar Institute, 2021a,b). These analyses completed the digital cartographic assessment and were further complemented by field-based surveys.

For small-scale gully erosion monitoring in Hiorthhamn, topographic surveys were made during field trips in late August/early September in 2019 and 2020. The timing was chosen to capture the end of summer situation, with the deeper active-layer depths and after the initial geomorphological activity during the development of an active layer. The surveys were made with a Trimble S5Series Motorized total station and a Trimble TSC3 controller; detailed point coordinates along each gully limit and thalweg were measured. The data acquired was used to calculate some basic scale (L_t – length, D_h – horizontal distance, L_d – length between gully head and gully mouth, H – height,) and shape parameters (C_v – vertical curvature, G_a – average gradient, A – area) (Table 1) (Ding et al., 2017). The three gullies were specifically chosen for monitoring due to their location in the proximity of fragile cultural heritage.

Cultural heritage data was retrieved from the online Norwegian national heritage database – Askeladden, Riksantikvaren (2021). The study area has 872 cultural heritage sites, which are registered as points; and an additional 100-m buffer area around each one of them, according to Svalbard Environmental Protection Act. This dataset was used to

Table 1
Parameters which describe scale and shape parameters of longitudinal gully profiles.

Parameter	Formula and description
<i>Lt</i> Length (m)	The length of the gully thalweg between the gully head and mouth. A longer <i>Lt</i> indicates that the gully has experienced a much longer development time and the erosion degree has been stronger (calculated in ArcGIS)
<i>Dh</i> Horizontal distance (m)	The horizontal distance from the gully head to mouth along the gully bottom. <i>Dh</i> can reflect development time and the erosion degree of the gully, similar to <i>Lt</i>
<i>Ld</i> Length between gully head and mouth (m)	The straight line between the gully head and mouth (calculated in ArcGIS)
<i>H</i> Height (m)	The vertical distance between the gully head and mouth; the greater <i>H</i> value, the higher potential energy is, meaning the gully may be in a relatively active stage (calculated in ArcGIS)
<i>Cv</i> Vertical curvature	$Cv = Lt/Ld$ ($Cv \geq 1$); in order to describe the curvature of the longitudinal profile. If <i>Cv</i> value is close to 1, the gully longitudinal profile is close to a straight line shape. Higher <i>Cv</i> values indicate a higher topographic relief (calculated in Excel)
<i>Ga</i> Average gradient	$Ga = H/Dh$ reflects the average slope of the longitudinal profile. For a gully with a given length, the larger <i>Ga</i> value, the greater <i>H</i> , and a larger <i>Ga</i> and greater <i>H</i> show that the gully is in an active stage and erosion is severe (calculated in Excel)
<i>A</i> Area (m ²)	Gully area calculated in ArcGIS with <i>Measure Tool</i>

Table 2
Sediment and lithotypes that underlying thermo-erosion gullies in Norden-skiöld Land.

Acronym	Lithology	Geological formation
MOR	Unconsolidated glacial till	/
MAD	Unconsolidated marine deposits	/
GFD	Unconsolidated glacio-fluvial deposits	/
SHS	Shale, sandstone	Frysjaodden
SND	Sandstone	Frysjaodden
GSD	Sandstone	Grumantbyen and Hollendardalen
SMS	Shale, mudstone, siltstone	Basilika
SSC	Sandstone, shale, coal	Firkanten
CSS	Shale, siltstone, sandstone	Carolinefjellet
SBT	Shale (bituminous), siltstone, sandstone	Janusfjellet Subgroup
DKS	Dark shale, siltstone, sandstone	Rurikfjellet
ASB	Shale (bituminous), siltstone	Agardhfjellet
STS	Shale, siltstone, sandstone	Storfjorden Subgroup
MBC	Mudstone (bituminous), calcareous siltstone	Botneheia
BMB	Mudstone (bituminous), siltstone, sandstone	Bravaisberget
SSL	Shale, siltstone	Vikingshøgda
KSC	Shert, siliceous shale, sandstone, limestone	Kapp Starostin
CRK	Carbonate rocks	Wordiekammen
SSH	Sandstone, shale	Orustdalen
DMC	Diamictite	Bellsund Group
QMD	Quartzite, metapelite, diamictite	Lågneset
MPQ	Phyllite, quartzite	Gåshamna
DLS	Dolomite, limestone, subordinate phyllite	Höferpynten

check how many CH sites (along with buffer areas) intersect with a gully, and it was made with the help of the *Intersection tool* from ArcGIS.

4. Results

4.1. Thermo-erosion gullies data analysis

A total of 810 TEG were digitised. They are represented as points in Fig. 3a. Different types of thermo-erosion gullies were mapped; a few examples are shown in Fig. 3b, c, d, e, f, g. Following the density analysis performed, the highest density (Fig. 4a) of thermo-erosion gullies is found north-east from Barentsburg, along the shore between Heerodden and Kapp Laila and Hollendardalen valley. This area is followed by the three second-densest areas located in Sassendalen (north-eastern part of Nordenskiöld land), on the shores of Van Muydenbukta bay and on the land slip between Kapp Morton and Svartodden (in the south-east). The large majority of the thermo-erosion gullies are located along the coastline. Judging by their area density (Fig. 4b), the largest thermo-erosion gullies occur at the highest density point, located at the mouth of Hollendardalen valley.

As previously highlighted by Nicu et al., 2021b the highest cultural heritage densities occur around the main human settlements in Long-yearbyen (Adventdalen), Barentsburg (Grønfjorden), and Colesbukta (Colesdalen).

As for the FAD of thermo-erosion gullies (Fig. 5), a size distribution that is quite similar to the FAD of a landslide inventory were obtained. The power-law exponent (β) of the inventory was calculated as ~ 2.5 , which is also similar to the values suggested for subaerial landslide inventories (i.e., $\beta_{\text{mean}} = 2.4\text{--}2.5$; Malamud et al., 2014; Tanyas et al., 2018). Fig. 5 also shows that the FAD diverges from the power-law towards the small gullies, which bears similarities with landslide inventories. We should stress that these similarities should not be attributed to the same physical explanations. For instance, variation from high to low frequencies observed from small to large landslides, on one hand, is associated with the transition from shear resistance controlled by cohesion to friction, respectively (e.g., Bennett et al., 2012). On the other hand, gullies are enlarged as a result of gradual surface processes and therefore, large gullies are, in fact, expanded versions of small ones. However, taking aside the similarities between FADs of landslides and gullies, examining the FADs of more gully inventories would help us to understand if there is a specific ratio (i.e., a specific range for β) between the frequencies of small and large gullies. If this is the case, understanding the factors governing β could lead to developing more robust hazard assessment studies in terms of gully erosion.

The FAD shown above essentially provides an overview on the number of small to large gullies within a study area. But, as the traditional visualization is based on logarithmic scale, the actual distribution of the gully dimensions in the metric system is lost. For this reason, we also provide an overview of the gully area distribution in their original scale and complement this information with two additional morphometric characteristics, these being the maximum distance and the elongation index. These three parameters are shown in Fig. 6 where, as in many other natural processes, the respective distributions appear to be heavy-tailed. This is particularly true for the gully area, with a distribution that features large numbers of small gullies with a surface of around 500 m², and a progressive number of fewer gullies of medium to large sizes, up to a maximum close to 6000 m². Interestingly, the distributions of the two additional parameters computed are still positively skewed but more and more light-tailed. The bulk of the maximum gully distance (Fig. 6, central panel) distribution is approximately 30 m in length and only a few have matured into landforms with lengths greater than 300 m within this timeframe. To make matters more complex, the timeframe has varied since the gullies are often situated on isostatically uplifted previous marine deposits with varying age of uplift over the sea level.

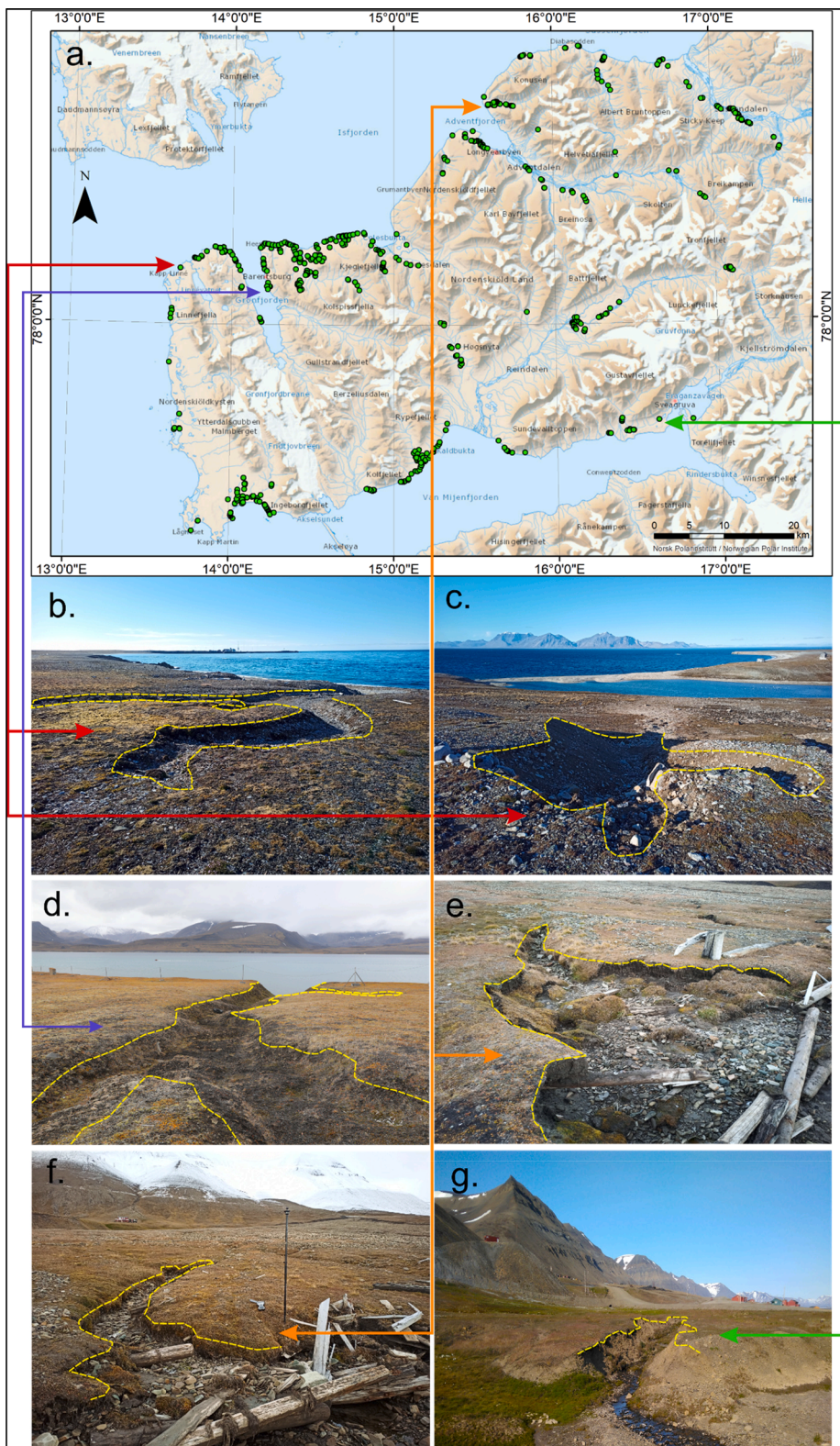


Fig. 3. a. Mapped thermo-erosion gullies in the study area represented as point features. A few examples of different types of thermo-erosion gullies on Svalbard; b. Gully cut into old raised beach deposits (Isfjord Radio in the background); c. Gully cut into uplifted beach and marine deposits at the mouth of Linnéelva river close to the CH at Russekeila; d. Gully cut into uplifted beach deposit at Finneset (next to Barentsburg); e, f. Gullies cut into the fluvial fan surface at Hiorthhamn (Adventfjorden) affecting cultural heritage remains from mining industry; g. Gully located in the proximity of Svea cut into raised marine deposits with soliflucted surface.

As for the shape of the gullies, most of them appear to have an elongation index of 2.2 (Fig. 6, right panel). This value implies that their shape tends to be rounded and only few cases reach elongation indices above 5, a threshold marking very elongated landforms. The information these three plots convey supports the statement that the genesis of gullies in Nordenskiöld Land is predominantly recent. Before describing the results of the field surveys though, we opted to summarize the

distribution of terrain characteristics at locations with or without gully occurrences.

4.2. Terrain factors characterising thermo-erosion gullies in Nordenskiöld Land

Results from the terrain factor analysis is shown in Fig. 7 where

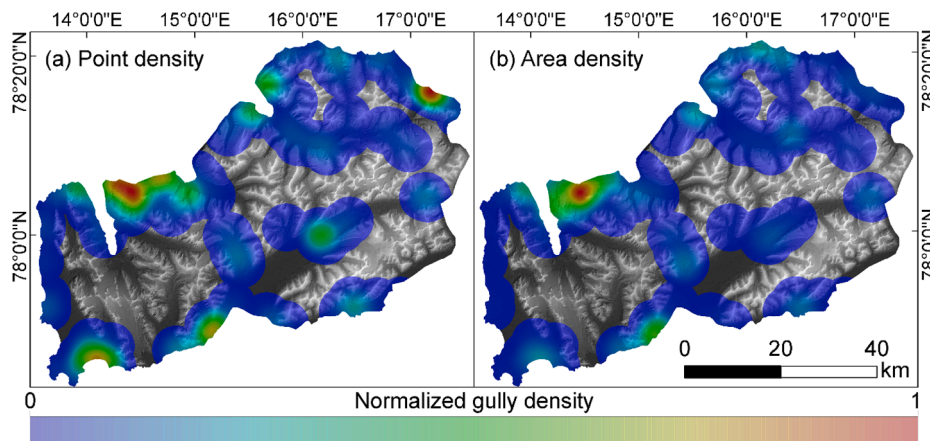


Fig. 4. The normalized gully density for the study area by: a. point; b. area.

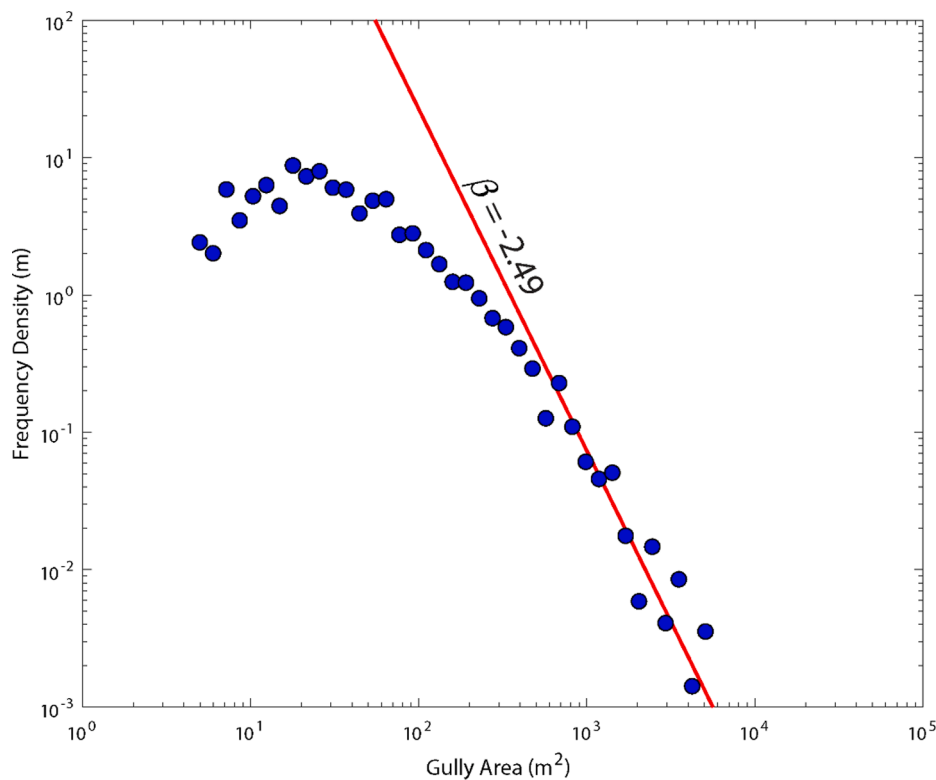


Fig. 5. The frequency area distribution (FAD) obtained for TEG inventory in Nordenskiöld Land.

marked differences in the distribution of terrain characteristics between locations labelled as NG (No-Gully) and G (Gully), are indicators of environmental attributes that favour gully occurrences. We stress here that to extract the G information, we have created a buffer of 30 m around each TEG polygon, subtracting the TEG surface itself. This implies that the terrain characteristics we report in Fig. 7 for gully presences are diagnostic of the relatively stable neighbourhood where the gully initiated, which we investigated thanks to a 5 m resolution DEM. For each buffer, we then computed the mean of each terrain parameter, whereas for the NG cases, we used the whole distribution across the study site.

For the Elevation, the bulk of the gullies are in the range between the sea level and 50 m a.s.l., with a few exceptions up to around 200 m a.s.l. Conversely, Eastness and Northness show a similar exposition distribution in both cases, although gullies are slightly more predominant on Eastward and Northward facing slopes. An interesting situation is shown

by looking at the Elevation, Slope and Topographic Roughness because these three parameters convey part of the very same spatial signal but also bring something different at the same time. For instance, no gully occurs at elevations greater than 200 m a.s.l., but gullies occur up to a maximum steepness of 37 degrees and generally in a mildly rough terrain.

As for the influence of the terrain curvatures, these appear to be also of less relevance. This is particularly true for the profile curvature (PRC) whereas in the case of planar curvature (PLC), the distribution of PLC values extracted at locations where thermo-erosion gullies occur predominantly shows negative (laterally concave) and zero (linear surface) values. This implies that there are no gullies where PLC is positive (laterally convex).

Morphologically, this is coherent with what we expect from a geomorphological standpoint for landforms that tend to exhibit negative planar curvatures correspond to landscape incisions where gullies

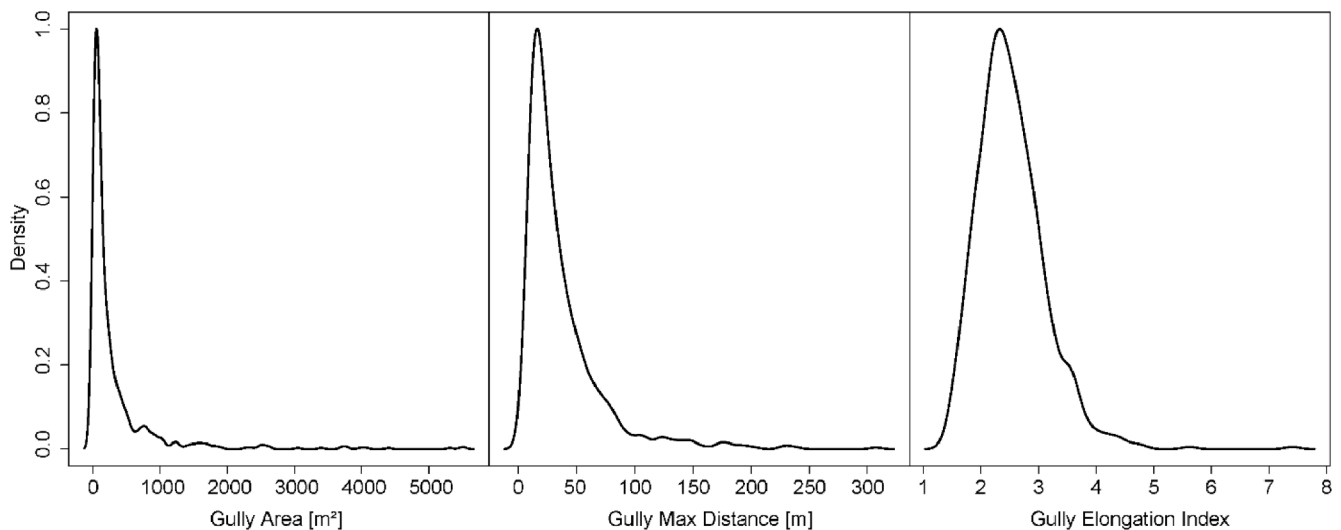


Fig. 6. Probability density functions obtained for three TEG parameters: gully area (left panel), gully maximum distance (central panel), and gully elongation index (right panel).

naturally initiate and develop. Conversely, positive PLC values are diagnostic of terrains where water diverges rather than converge, limiting the surface incision, a condition for the genesis of thermo-erosion gullies. Ultimately, we also tried to investigate whether underlying lithologies predispose the occurrence of thermo-erosion gullies. This attempt is challenging since there is no coherent dataset over unconsolidated sediments or bedrock lithologies on Svalbard, but only a composite, where areas with thick unconsolidated sediments (class MOR, MAD and GFD) are only coarsely defined, but the same area are lacking lithological information. In the same way areas with shale dominated lithology are so physically weathered by the harsh Arctic climate that the residual material have mechanical properties similar to unconsolidated sediments.

Fig. 8 highlights that thermo-erosion gullies are predominant in unconsolidated substrata (MAD and GFD). This is logical since unconsolidated sediments have open pore-spaces, which is the base for high accumulation of internal ice in permafrost regions, and hence vulnerable to thermo-karst processes during thawing seasons. This may also be due to the natural spatial distribution of these parent materials in the lower elevations of the landscape. They mainly occur along valley bottoms and the coastline where the combined action of fluvial and coastal erosion and thermal variations may destabilize the soil leading to the genesis of thermo-erosion gullies.

Aside from unconsolidated sediments, the underlying lithotypes with the highest frequency of gullies are sandstones (SND) and shale-rich parent materials (SMS and CSS). The former lithotype will, as climate induces rapid surface weathering, alter the grain-to-grain bond, tend to produce loose soil columns, which can be mobilized with relative ease as permafrost thaws. Shale-rich bedrock have the added instability of giving rise to clayey soils which are naturally weak to variations in water content. As permafrost thaws is releasing water into the soil; this is combined with the swelling effect of clay minerals to rapidly reduce stability in the sediment.

4.3. Monitoring of small-scale gully erosion

The results of the monitoring of three small-scale fluvial gullies are shown in Fig. 9. The gullies are located on the north-eastern shores of Adventfjorden, approximately 3 km north of Longyearbyen (Fig. 9a), at the mouth of Telegrafdalen river. Limits (Fig. 9b) and main characteristics of the three gullies are shown in Table 3.

During the two years monitoring, there were very few changes in the gullies morphology. The length (L_t) varies between 10.7 and 16.65 m for

gully number 01 and gully number 02, respectively. It can be observed that the length of the gullies has diminished from 2019 to 2020 monitoring. This is due to the fact that there is a lot of sorted and unsorted material coming down from the fluvial system upstream, filling up the gully depression. This happens during short term episodes of high energy surface overland flow. Also, being close to the coastline, the gullies are under the effect of the tides, which is also transporting sand and driftwood into the gullies; hence, influencing the thalweg length of the gully. L_t has a similar effect on the L_d , which has also decreased (Table 3). There was no significant gully head advancement for the three gullies, except for gully number 01, which advanced with 0.5 m in one year. (Fig. 9b).

The same tendency can be observed for the H , which has also decreased for all gullies. C_v values are all close to 1, which shows the fact that the gullies longitudinal profile is close to a straight line shape, which is also visible in Fig. 8b. G_a values are low, indicating the fact that the gullies are not very active, and the erosion is not severe. Regarding the A of the gullies, there has been an increase; this is due to the lateral collapses, especially for the gully 01 and 02 (Fig. 9b). These lateral collapses seems to be due to undercutting through high tide/wave induced action in the lower parts of the gully.

4.4. Cultural heritage analysis

The majority of Svalbard's CH are located in the coastal area (Nicu et al., 2021b). Following the *Intersection* analysis, out of 872 CH sites, 44 sites (Supplementary material 1) were found to be vulnerable to future evolution of TEG; out of 44 CH sites, 29 are also exposed to coastal erosion and three to river erosion. They are mainly located near the two main settlements, Longyearbyen and Barentsburg, and Colesbukta.

The grave visible in Fig. 10a is located in Finneset, at approximately 1 km SSE from Barentsburg. The description of the grave is as follows "well-defined grave, located between two brooks in a flat area about 20 m from the shoreline; the grave is oriented E-W, with well-preserved cross. The grave is covered with a thick rope, about 40 cm high with sharp edges" (Askeladden, Riksantikvaren, 2021). The description could be more precise (with some additional information observed in the field during the summer of 2021), also referring to the landscape around the cross; the two "brooks" are actually two well-separated active gullies of considerable size. The one in the northern part has a length of about 165 m and the one in the southern part a length of about 155 m. The cross itself is also vulnerable to coastal erosion.

The house remains from Fig. 10b are described as "rectangular house

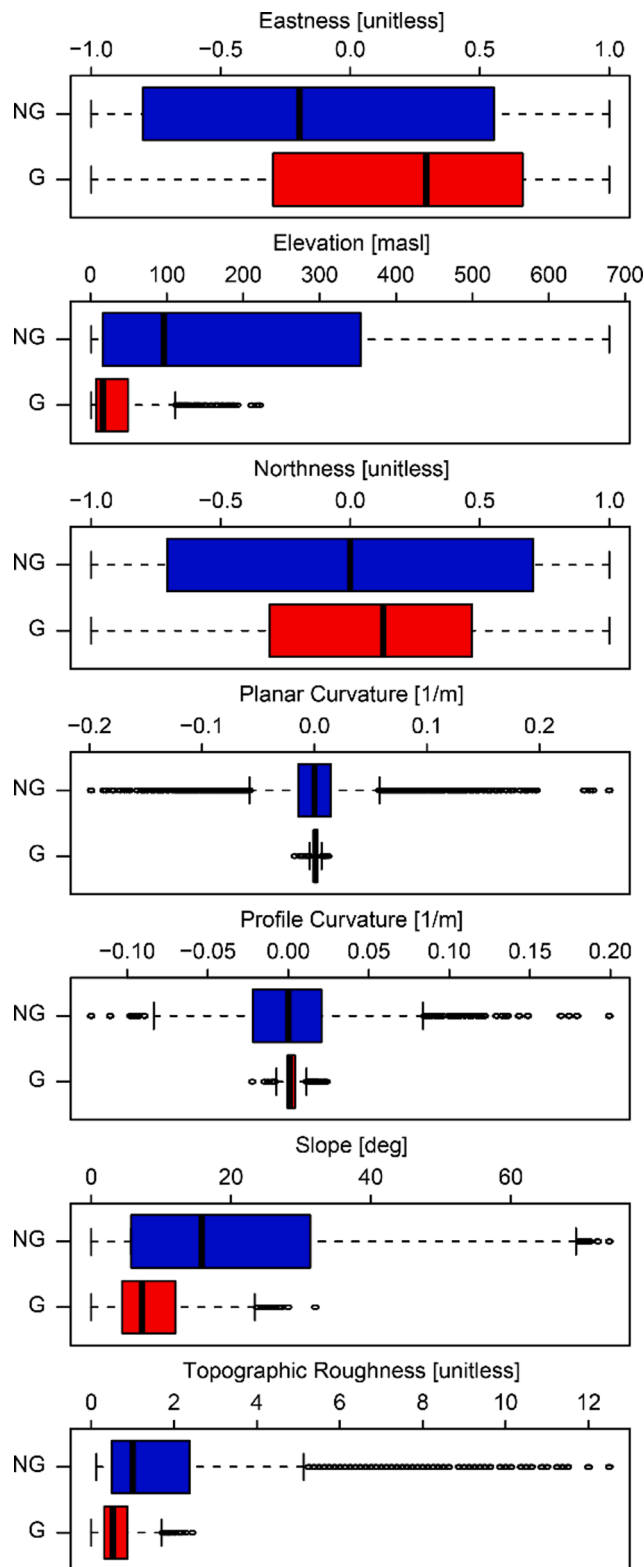


Fig. 7. Summary statistics of terrain properties at locations where TEG are present (G) and absent (NG).

remnant, oriented E-W. The house is marked as a burial in the ground with remnants of peat walls, walls of 30 cm wide, 20 cm high and 10 cm in depth. Remains of dry vertical logs of 50–100 cm in height” (Askeladden, Riksantikvaren, 2021). This is located approximately 125 m SSW from the grave, on the south part of the 165 m gully. Also vulnerable to coastal erosion.

The Security Zone (Fig. 10c) has no description; however, this refers to the 100 m buffer zone around a protected cultural heritage site, in this case the remains of the cable car that used to transport coal in the past (Fig. 10f). The security zone is also vulnerable to coastal erosion (Jaskólski et al., 2018).

The remains of the road (Fig. 10d) are described as “the road from Skjæringa to the preparation plant; it was built in 1967 and was in use until 1985, when a new road was built closer to the sea. The road is built up on the terrain and gravelled. A possible theory of the name may be that it originates from a steep road” (Askeladden, Riksantikvaren, 2021). The new road refers to the present day road that is connecting Longyearbyen to the Longyearbyen airport.

The plane wreck in Adventdalen (Fig. 10e) is described as “remains of wings and cockpit, scattered remains in the area around” (Askeladden, Riksantikvaren, 2021). No further details were provided. However, more details were found about the context of the plane wreck. In the past, planes were landing in Adventdalen (the old airport), about 4 km east of Longyearbyen, until the new airport at Hotellneset was built in 1973 and opened in 1975. The wreck is represented by a German Ju 88, which on June 14, 1942, flying from Banak in north Norway landed on the airstrip in Adventdalen; it was damaged because the ground was soft. Almost two weeks later, it was seriously damaged during an attack by an allied Catalina; following this, it was left behind. Today, the wreck of the German Ju 88 is very close to Adventelva River (Stange, 2019) (as visible in the background of Fig. 10e). Besides the gully that is visible in the foreground of Fig. 10e, the wreck is vulnerable to Adventelva river erosion.

5. Discussion

There is an immediate need to study the implications of climate-induced geomorphological processes and hazards in the Arctic with the potential to affect cultural heritage sites. One such relevant process is thermo-erosion gullying, which can be postulated to be increasingly active under a warming climate (Godin et al., 2019). Literature has shown that the peak of erosion rate and enlargement of a gully occurs during the first part of its entire lifetime (Sidorchuk, 1999, 2006). Godin et al., 2014 study from Canada showed that active gullying triggered not only a change in drainage pattern but also more efficient drainage of the neighbouring wetlands; moreover, a stabilised state was usually reached between 5 and 10 years after the initial incidence of erosion. It was shown that gullies were often co-existing with thaw slumps, sinkholes and tunnels and that their erosion rates were highly variable over the last four decades (1972–2007); with mean values of 4.39 m y^{-1} in length and $61.4 \text{ m}^2 \text{ y}^{-1}$ in area. In this study, we were not able to provide such long-term analysis, taking into consideration that our main data set comes from only one set of spatial observations. As soon as new high resolution spatial data becomes available (the present ones are from 2009 to 2011), a spatio-temporal analysis will be made. Also, the Godin et al., 2014 erosion rates are not comparable with the ones from the one-year small-scale gullying monitoring that was made.

The Devon Island study found that: gullies are found on all slopes, regardless of orientation; geology has a significant role in gully initiation, development and morphology, especially geological formations dolostone and limestone. In this study, we find that sandstones are dominant of the solid bedrock lithologies, while in Nordenskiöld Land, slopes oriented towards north, and east are more favourable to gully initiation and development. The distribution of gullies only under 200 m a.s.l. in this study points to the importance of the substrate (sediment) for gully formation. Central Svalbard has experienced an *iso*-static rebound of up to 65–70 m after the last ice-age (Lønne, 2005) – meaning areas under this elevation often have a marine-originating sediment cover. The lower valleys in this paraglacial landscape are also the sites for both glacial- and glacio-fluvial sediment deposition, while higher areas are exhibiting more bare rocks, slope process deposits and in situ weathering material.

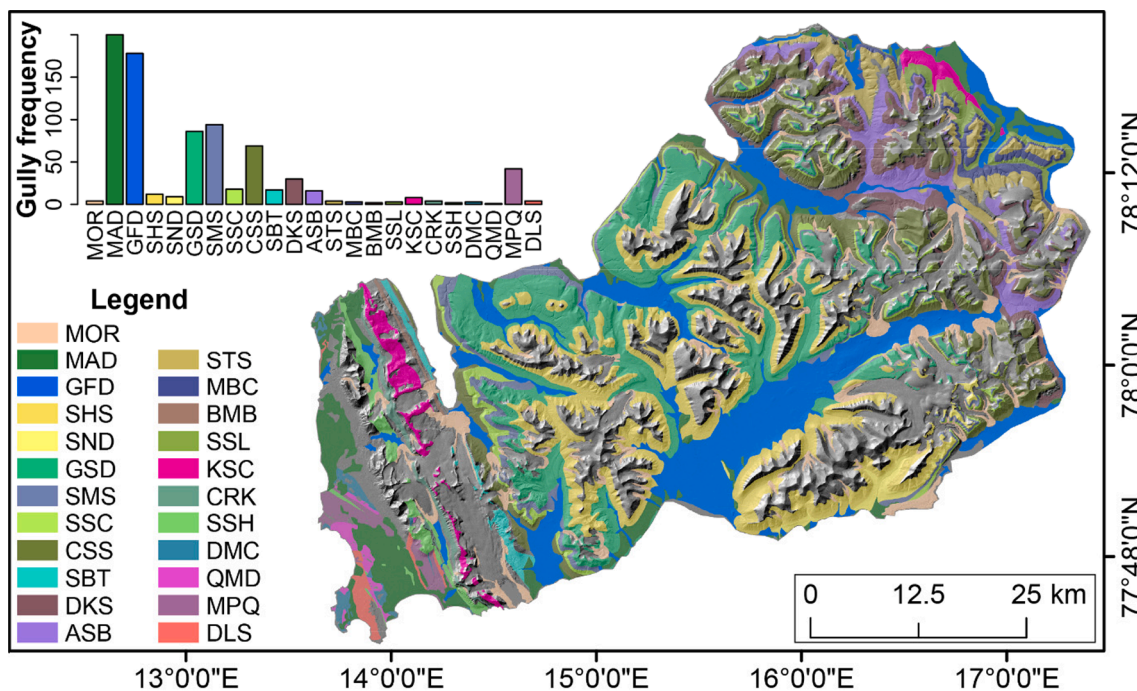


Fig. 8. The panel from the upper left part reports the number of gullies per underlying lithological class, whereas the map shows the corresponding lithotypes across Nordenskiöld Land. The lithotypes corresponding to the acronyms in this figure are reported in Table 2 (here we show only the underlying bedrock for the gullies, leaving other lithotypes unmarked).

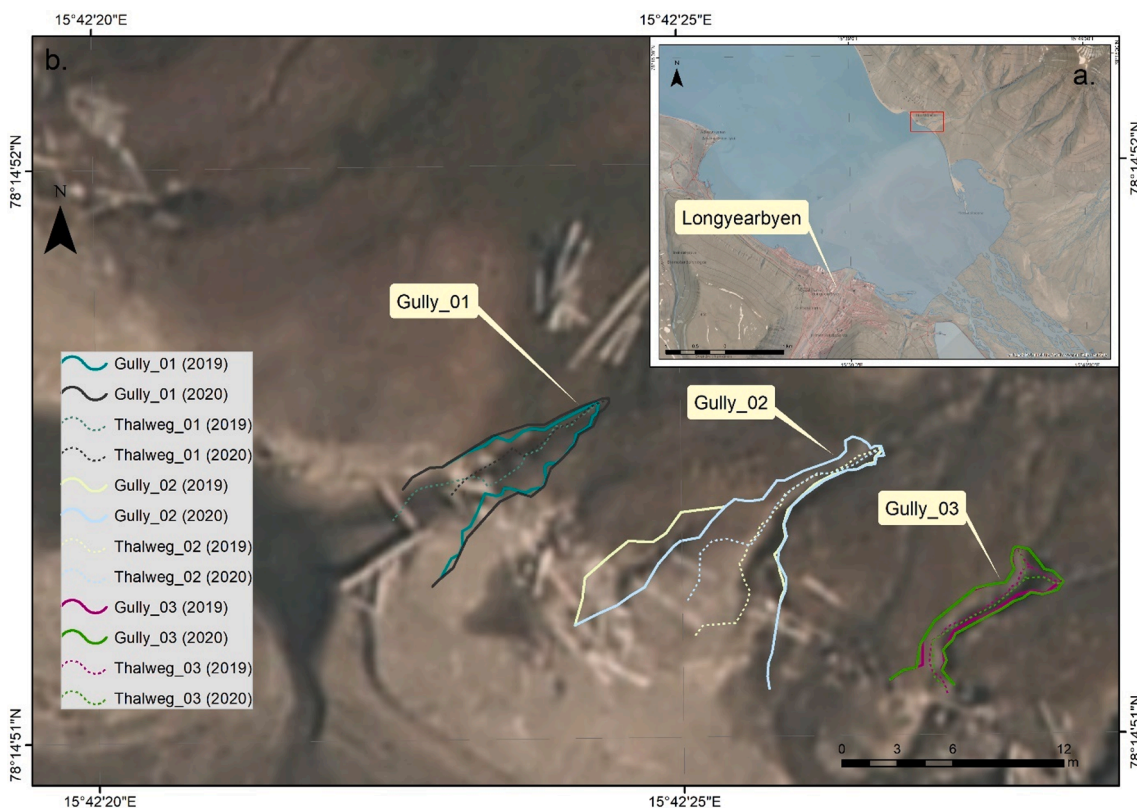


Fig. 9. a. General location of the three gullies; b. Details of the gully limits and thalweg (background image from Norwegian Polar Institute).

Sidorchuk, 2020 study from Russia (Yamal Peninsula) revealed highly uneven distribution of erosion potential level with the maximums on steep banks of the river valleys and in gully heads; moreover, the erosion potential was linked to landforms with steep slopes and unstable

vegetation cover. Anthropogenic interventions, such as railways, roads and pipelines were also found to influence the initiation and development of gullies. In our case, gullies can be found on up to 37 degrees slopes and numerous gullies are developed around the two main

Table 3
Scale and shape parameters of the three gullies.

Parameters / Year	Gully_01		Gully_02		Gully_03	
	2019	2020	2019	2020	2019	2020
<i>Lt</i> (m)	14.1	10.7	16.65	13.77	12.13	11.13
<i>Dh</i> (m)	14.1	10.7	16.65	13.77	12.13	11.13
<i>Ld</i> (m)	12.8	10.06	14.45	12.17	8.75	8.62
<i>H</i> (m)	0.72	0.93	1.73	1.51	1.34	1.19
<i>Cv</i> (unitless)	1.10	1.06	1.15	1.13	1.38	1.29
<i>Ga</i> (unitless)	0.05	0.08	0.10	0.10	0.11	0.10
<i>A</i> (m ²)	33.09	38.31	69.63	83.46	14.63	16.09

settlements – Longyearbyen and Barentsburg. At this point, however, it cannot be concluded whether direct physical anthropogenic interventions has had a significant contribution to the initiation and development of gullies.

Gullies are landforms that widen and lengthen in time as land degradation takes place (in this case laterally thawing of permafrost). And the very fact that most of the mapped gullies are small, short and rounded in overall shape supports the hypothesis that they still have a large potential to mature. These considerations are valid looking at the study area as a whole and a detailed assessment is required to confirm or reject this hypothesis. Other considerations would be to look and try to

detect the time the gullies have been active and try to detect any on-off mode in activity, for example triggered by interchanging warmer and colder periods, especially concerning the lengths of thawing seasons and maybe maximum summer temperatures. This is however difficult since spatial data, aerial and satellite photographs are sparse in time and space over the arctic back in time.

Further research is needed on Svalbard's thermo-erosion gullies, especially regarding the spatio-temporal development and connection to sediment types, to better understand local and regional factors controlling distribution and future development. Understanding the large-scale pattern represents a future research direction, along with continuing the small-scale gully erosion monitoring. Another future research direction is towards (multi)hazard predictive modelling of Arctic thermo-erosion gullies and retrogressive thaw slumps, given the logical link between thermal-gully initiation and activity, and arctic climate warming caused by the geomorphological mechanism linked to the thickness of active layers in permafrost regions.

The here presented thermo-erosion gully inventory is valuable when regarded from a climate change perspective, as it can be utilised by scientists from various backgrounds, such as cryosphere research, geomorphology, statistical modelling of climate-induced geomorphological processes, hydrologists, cultural heritage planners, etc. The inventory and maps also represent a new standalone dataset of high importance for

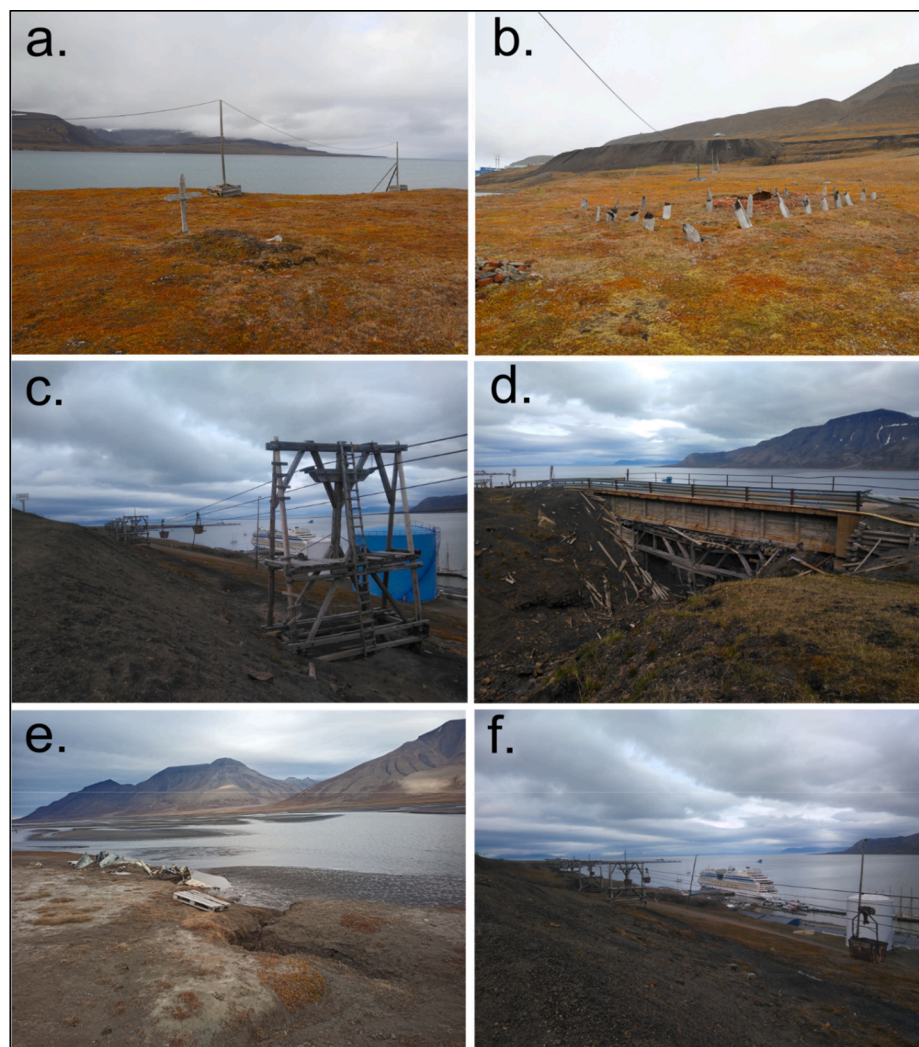


Fig. 10. Details of various cultural heritage sites primarily endangered by gully erosion and other associated processes; a. Remains of a grave in the proximity of Barentsburg; b. Remains of a telecommunication cabin in the proximity of Barentsburg; c. Security zone located west of Longyearbyen; d. Remains of mining exploitation road; e. Wrecks of an airplane located in Adventdalen; f. Coal industry cable car remains along the Longyearbyen port.

both local, regional and international context and can be used in future spatio-temporal analyses and/or multi-hazard assessment of climate-induced processes (Lombardo et al., 2020; Saha et al., 2021; Javidan et al., 2021). The accumulation and combination of these types of datasets could have a high impact on mitigating climate change effects on pan-Arctic infrastructure (Hjort et al., 2018) and Arctic cultural heritage landscapes (Nicu et al., 2021b; Thuestad et al., 2015, 2021). As Arctic cultural heritage landscapes represent a projection of the past, it is in our moral responsibility to try to protect and preserve them.

6. Conclusions

Nordenskiöld Land, Svalbard represents a typical Arctic permafrost landscape with a multitude of unique cultural heritage sites and remnants, which has not previously been studied for thermo-erosion gully hazards. We present for the first time a comprehensive dataset of 810 gullies in this area, their general topographical and lithological setting, together with a spatio-statistical analyses comparing them with protected and vulnerable cultural heritages in the same area. We also present some observations and hypothesis into geographically and sedimentological controlling factors of thermo-erosion gully activity and spatial distribution, together with an initial short-term small study monitoring of small-scale gully. The results so far indicate that thermo-erosion gullying and cultural heritage in Nordenskiöld land co-exists on a regional level, although direct erosion and hazard for CH is not yet at any critical scale. The spatial coastal and low-land focus of both thermo-erosion gullies and CH however gives reason for future concern. A rapidly warming Arctic climate would favour increased permafrost active layer thickness and hence potential accelerated thermo-erosion gullying in susceptible areas, which we show overlap with the highest CH densities. Although not conclusive in understanding present and future development of thermo-erosion gullying, this study underpins the relevance and importance of geohazard mapping and research in Arctic settings where CH and present human activity and infrastructure is the most vulnerable to increasingly rapid changes in natural physical and geomorphological conditions and processes.

Declaration of Competing Interest

The authors declare that they have no known competing financial interests or personal relationships that could have appeared to influence the work reported in this paper.

Acknowledgements

This work was partially financed by the Fram Center flagship Klimaeffekter på økosystemer, landskap, lokalsamfunn og orfolk grant nr. 369913 and nr. 369924, GEOCULT – Monitoring Geohazards Affecting Cultural Heritage Sites at Svalbard. Many thanks to Adrian Pop, which was a very reliable polar bear guard during the field trip to Barentsburg. James S. Williamson (Memorial University of Newfoundland, Canada) is kindly acknowledged for the English language editing of the manuscript.

References

- Askeladden, Rikskontrollvaren – Norwegian Directorate for Cultural Heritage Management. Available online at <https://www.rikskontrollvaren.no/veiledere/askeladden/> (accessed 25 May 2021).
- Azareh, A., Rahmati, O., Rafiei-Sardooi, E., Sankey, J.B., Lee, S., Shahabi, H., Ahmad, B. B., 2019. Modelling gully-erosion susceptibility in a semi-arid region, Iran: Investigation of applicability of certainty factor and maximum entropy models. *Sci. Total Environ.* 655, 684–696. <https://doi.org/10.1016/j.scitotenv.2018.11.235>.
- Bartsch, A., Höfler, A., Kroisleitner, C., Trofaiar, A.M., 2016. Land Cover Mapping in Northern High Latitude Permafrost Regions with Satellite Data: Achievements and Remaining Challenges. *Remote Sens.* 8, 979. <https://doi.org/10.3390/rs8120979>.
- Bennett, G.L., Molnar, P., Eisenbeiss, H., Mc Ardell, B.W., 2012. Erosional power in the Swiss Alps: characterization of slope failure in the Illgraben. *Earth Surf. Proc. Land.* 37 (15), 1627–1640. <https://doi.org/10.1002/esp.3263>.

- Berthling, I., Berti, C., Mancinelli, V., Stendardi, L., Piacentini, T., Miccadei, E., 2020. Analysis of the paraglacial landscape in the Ny-Ålesund area and Blomstrandøya (Kongsfjorden, Svalbard, Norway). *J. Maps* 16 (2), 818–833. <https://doi.org/10.1080/17445647.2020.1837684>.
- Bintanja, R., 2018. The impact of Arctic warming on increased rainfall. *Sci. Rep.* 8, 16001. <https://doi.org/10.1038/s41598-018-34450-3>.
- Biskaborn, B.K., Smith, S.L., Noetzi, J., Matthes, H., Vieira, G., Streletskiy, D.A., Schoeneich, P., Romanovsky, V.E., Lewkowicz, A.G., Abramov, A., Allard, M., Boike, J., Cable, W.L., Christiansen, H.H., Delaloye, R., Diekmann, B., Drozdov, D., Etzelmüller, B., Grosse, G., Guglielmin, M., Ingeman-Nielsen, T., Isaksen, K., Ishikawa, M., Johansson, M., Johansson, H., Joo, A., Kaverin, D., Kholodov, A., Konstantinov, P., Kröger, T., Lambiel, C., Lanckman, J.-P., Luo, D., Malkova, G., Meiklejohn, I., Moskalenko, N., Oliva, M., Phillips, M., Ramos, M., Sannel, A.B.K., Sergeev, D., Seybold, C., Skryabin, P., Vasiliev, A., Wu, Q., Yoshikawa, K., Zheleznyak, M., Lantuit, H., 2019. Permafrost is warming at a global scale. *Nat. Commun.* 10 (1) <https://doi.org/10.1038/s41467-018-08240-4>.
- Bogolyubova, N., Nikolaeva, Yu., Portnyagina, M., Elts, E., 2019. International Cooperation in the Arctic as a Way to Preserve the Natural and Cultural Heritage. *IOP Conf. Ser.: Earth Environ. Sci.* 302, 012054 <https://doi.org/10.1088/1755-1315/302/1/012054>.
- Borrelli, P., Robinson, D.A., Fleischer, L.R., Lugato, E., Ballabio, C., Alewell, C., Meusburger, K., Modugno, S., Schütt, B., Ferro, V., Bagarello, V., Oost, K.V., Montanarella, L., Panagos, P., 2017. An assessment of the global impact of 21st century land use change on soil erosion. *Nat. Commun.* 8 (1) <https://doi.org/10.1038/s41467-017-02142-7>.
- Chen, J., Liu, L., Zhang, T., Cao, B., Lin, H., 2018. Using Persistent Scatterer Interferometry to Map and Quantify Permafrost Thaw Subsidence: A Case Study of Eboiling Mountain on the Qinghai-Tibet Plateau. *J. Geophys. Res.-Earth* 123 (10), 2663–2676. <https://doi.org/10.1029/2018JF004618>.
- Christensen, T.R., Lund, M., Skov, K., Abermann, J., López-Blanco, E., Scheller, J., Scheel, M., Jackowicz-Korczynski, M., Langley, K., Murphy, M.J., Mastepeanov, M., 2021. Multiple ecosystem effects of extreme weather events in the Arctic. *Ecosystems* 24 (1), 122–136. <https://doi.org/10.1007/s10021-020-00507-6>.
- Ciampalini, A., Frodella, W., Margottini, C., Casagli, N., 2019. Rapid assessment of geohydrological hazards in Antananarivo (Madagascar) historical centre for damage prevention. *Geomat. Nat. Haz. Risk* 10 (1), 1102–1124. <https://doi.org/10.1080/19475705.2018.1564375>.
- Clauset, A., Shalizi, C.R., Newman, M.E.J., 2009. Power-Law Distributions in Empirical Data. *SIAM Review* 51 (4), 661–703. <https://doi.org/10.1137/070710111>.
- Collard, F., Husum, K., Eppé, G., Malherbe, C., Hallanger, I.G., Divine, D.V., Gabrielsen, G.W., 2021. Anthropogenic particles in sediment from an Arctic fjord. *Sci. Total Environ.* 772, 145575. <https://doi.org/10.1016/j.scitotenv.2021.145575>.
- Dahle, K., Bjørck, H.B., Prestvold, K., 2000. Kulturminneplan for Svalbard 2000–2010. Cultural heritage plan for Svalbard 2000–2010. Longyearbyen, Governor of Svalbard, 2000. Sysselmannens Rapp. 2, 126. https://www2.sysselmannen.no/globalassets/sysselmannen-dokument/trykksaker/kulturminneplan_2am0y.pdf (accessed 6 May 2021).
- de Haas, T., Kleinhan, M.G., Carbonneau, P.E., Rubensdotter, L., Hauber, E., 2015. Surface morphology of fans in the high-Arctic periglacial environment of Svalbard: Controls and processes. *Earth Sci. Rev.* 146, 163–182. <https://doi.org/10.1016/j.earscirev.2015.04.004>.
- Demidov, N.E., Borisik, A.L., Verkulich, S.R., Wetterich, S., Gunar, A.Y., Demidov, V.E., Zheltenkova, N.V., Koshurnikov, A.V., Mikhailova, V.M., Nikulina, A.L., Novikov, A. L., Savatuygin, L.M., Sirotkin, A.N., Terekhov, A.V., Ugrumov, Y.V., Schirrmeister, L., 2020. Geocryological and hydrogeological conditions of the Western part of Nordenskiöld Land (Spitsbergen Archipelago). *Izvestiya, Atmospheric and Oceanic Physics* 56 (11), 1376–1400. <https://doi.org/10.1134/S000143382011002X>.
- Dickson, J., Head, J., Levy, J., Morgan, G., Marchant, D., 2017. Gully formation in the McMurdo Dry Valleys, Antarctica: multiple sources of water, temporal sequence and relative importance in gully erosion and deposition processes. In: Conway, S.J. (Ed.), *Martian Gullies and their Earth Analogues*. Geological Society of London, London. <https://doi.org/10.1144/SP467.4>.
- Ding, L., Qin, F.-C., Fang, H.-D., Liu, H., Zhang, B., Shu, C.-Q., Deng, Q.-C., Liu, G.-C., Yang, Q.-Q., 2017. Morphology and controlling factors of the longitudinal profile of gullies in the Yuanmou dry-hot valley. *J. Mt. Sci.* 14 (4), 674–693. <https://doi.org/10.1007/s11629-016-4189-7>.
- Ding, Y., Mu, C., Wu, T., Hu, G., Zou, D., Wang, D., Li, W., Wu, X., 2021. Increasing cryospheric hazards in a warming climate. *Earth Sci. Rev.* 213, 103500. <https://doi.org/10.1016/j.earscirev.2020.103500>.
- Elvevold, S., Dallmann, W., Blomeier, D., 2007. Geology of Svalbard. Norwegian Polar Institute; pp. 36. <https://brage.npolar.no/npolar-xmlui/bitstream/handle/11250/173141/GeologyOfSvalbard.pdf?sequence=1&isAllowed=y> (accessed 20 May 2021).
- Flyen, A.-C., Flyen, C., Mattson, J., 2020. Climate change impacts and fungal decay in vulnerable historic structures at Svalbard. *E3S Web of Conferences* 172, 20006. <http://doi.org/10.1051/e3sconf/202017220006>.
- Ford, J.D., Smit, B., Wandel, J., 2006. Vulnerability to climate change in the Arctic: A case study from Arctic Bay, Canada. *Global Environ. Chang.* 16, 145–160. <https://doi.org/10.1016/j.gloenvcha.2005.11.007>.
- Ford, J.D., Pearce, T., Villaverde Canosa, I., Harper, S., 2021. The rapidly changing Arctic and its societal implications. *Wires Clim. Change* 12, e735. <https://doi.org/10.1002/wcc.735>.
- Fortier, D., Allard, M., Shur, Y., 2007. Observation of Rapid Drainage System Development by Thermal Erosion of Ice Wedges on Bylot Island, Canadian Arctic

- Archipelago. *Permafrost and Periglac. Process.* 18, 229–243. <https://doi.org/10.1002/ppp.595>.
- Gales, J.A., Forwick, M., et al., 2013. Arctic and Antarctic submarine gullies—A comparison of high latitude continental margins. *Geomorphology* 201, 449–461. <https://doi.org/10.1016/j.geomorph.2013.07.018>.
- Godin, E., Fortier, D., 2012. Geomorphology of a thermo-erosion gully, Bylot Island, Nunavut. *Canada. Can. J. Earth Sci.* 49, 979–986. <https://doi.org/10.1139/e2012-015>.
- Godin, E., Fortier, D., Coulombe, S., 2014. Effects of thermo-erosion gully on hydrologic flow networks, discharge and soil loss. *Environ. Res. Lett.* 9, 1051010. <https://doi.org/10.1088/1748-9326/9/10/1051010>.
- Godin, E., Osinski, G.R., Harrison, T.N., Pontefract, A., Zanetti, M., 2019. Geomorphology of Gullies at Thomas Lee Inlet, Devon Island, Canadian High Arctic. *Permafrost and Periglac. Process.* 30, 19–34. <https://doi.org/10.1002/ppp.1992>.
- Gurbanov, E.A., Ganieva, S.A., 2017. Intensity of gully erosion in arid zone of Azerbaijan republic (by the example of the region of the Mingechaur water reservoir). *Arid Ecosyst.* 7, 251–255. <https://doi.org/10.1134/S2079096117040023>.
- Guzzetti, F., Reichenbach, P., Cardinali, M., Ardizzone, F., 2005. Probabilistic landslide hazard assessment at the basin scale. *Geomorphology* 72, 272–299. <https://doi.org/10.1016/j.geomorph.2005.06.002>.
- Hacquebord, L., 2001. Three centuries of whaling and walrus hunting in Svalbard and its impact on the Arctic ecosystem. *Environ. Hist.* 7, 169–180.
- Hagen, D., Vistad, O., Eide, N.E., Flyen, A.-C., Fangel, K., 2012. Managing visitor sites in Svalbard: from a precautionary approach towards knowledge-based management. *Polar Res.* 31, 18432. <https://doi.org/10.3402/polar.v31i0.18432>.
- Hanssen-Bauer, I. et al., 2017. Climate in Norway 2100 – a knowledge base for climate adaptation. Norwegian Centre for Climate Services report 1/2017.
- Hanssen-Bauer, I. et al., 2019. Climate in Svalbard 2100 – a knowledge base for climate adaptation. Norwegian Centre for Climate Services report 1/2019.
- Hjort, J., et al., 2018. Degrading permafrost puts Arctic infrastructure at risk by mid-century. *Nat. Commun.* 9, 5147. <https://doi.org/10.1038/s41467-018-07557-4>.
- Hollesen, J., Callanan, M., et al., 2018. Climate change and the deteriorating archaeological and environmental archives of the Arctic. *Antiquity* 92, 573–586. <https://doi.org/10.15184/aqy.2018.8>.
- Hovius, N., Stark, C.P., Allen, P.A., 1997. Sediment flux from a mountain belt derived by landslide mapping. *Geology* 25, 231–234. [https://doi.org/10.1130/0091-7613\(1997\)025<0231:SFFAMB>2.3.CO;2](https://doi.org/10.1130/0091-7613(1997)025<0231:SFFAMB>2.3.CO;2).
- Iwahana, G., Takano, S., Petrov, R.E., et al., 2014. Geocryological characteristics of the upper permafrost in a tundra-forest transition of the Indigirka River Valley, Russia. *Polar Sci.* 8, 96–113. <https://doi.org/10.1016/j.polar.2014.01.005>.
- Jaskólski, M.W., Pawłowski, L., Strzelecki, M.C., 2018. High Arctic coasts at risk—the case study of coastal zone development and degradation associated with climate changes and multidirectional human impacts in Longyearbyen (Adventfjorden, Svalbard). *Land Degrad. Dev.* 29, 2514–2524. <https://doi.org/10.1002/ldr.2974>.
- Jaskólski, M.W., 2021. Challenges and perspectives for human activity in Arctic coastal environments – a review of selected interactions and problems. *Miscellanea Geographica – Regional Studies on Development* 25, 127–143. <https://doi.org/10.2478/mgrsd-2020-0036>.
- Javidan, N., Kavian, A., Pourghasemi, H.R., Conoscenti, C., Jafarian, Z., Rodrigo-Comino, J., 2021. Evaluation of multi-hazard map produced using MaxEnt machine learning technique. *Sci. Rep.* 11, 6496. <https://doi.org/10.1038/s41598-021-85862-7>.
- Karjalainen, O., et al., 2019. Circumpolar permafrost maps and geohazard indices for near-future infrastructure risk assessments. *Sci. Data* 6, 190037. <https://doi.org/10.1038/sdata.2019.37>.
- Kinossian, N., 2020. Svalbard's Haunted Landscapes. *Nordlit* 45, 86–103. <https://doi.org/10.7557/13.5028>.
- Kociuba, W., Gajek, G., Franczak, L., 2021. A Short-Time Repeat TLS Survey to Estimate Rates of Glacier Retreat and Patterns of Forefield Development (Case Study: Scottbreen, SW Svalbard). *Resources* 10, 2. <https://doi.org/10.3390/resources10010002>.
- Kokelj, S.V., Jorgenson, M.T., 2013. Advances in Thermokarst Research. *Permafrost and Periglac. Process.* 24, 108–119. <https://doi.org/10.1002/ppp.1779>.
- Lara, M.J., Chipman, M.L., Hu, F.S., 2019. Automated detection of thermoerosion in permafrost ecosystems using temporally dense Landsat image stacks. *Remote Sens. Environ.* 221, 462–473. <https://doi.org/10.1016/j.rse.2018.11.034>.
- Li, H., Cruse, R.M., Liu, X., et al., 2016. Effects of topography and land use change on gully development in typical Mollisol region of Northeast China. *Chin. Geogr. Sci.* 26, 779–788. <https://doi.org/10.1007/s11769-016-0837-7>.
- Li, Z., Zhang, W., et al., 2020. Sustainable Development of Arid Rangelands and Managing Rainwater in Gullies. *Central Asia. Water* 12, 2533. <https://doi.org/10.3390/w12092533>.
- Liucci, L., Meelli, L., Suteanu, C., Ponziani, F., 2017. The role of topography in the scaling distribution of landslide areas: A cellular automata modeling approach. *Geomorphology* 290, 236–249. <https://doi.org/10.1016/j.geomorph.2017.04.017>.
- Ljungqvist, F.C., Seim, A., Huhtamaa, H., 2020. Climate and society in European history. *Wires Clim. Change* 12, e691. <https://doi.org/10.1002/wcc.691>.
- Lombardo, L., Tanyas, H., Nicu, I.C., 2020. Spatial modeling of multi-hazard threat to cultural heritage sites. *Eng. Geol.* 277, 105776. <https://doi.org/10.1016/j.enggeo.2020.105776>.
- Lousada, M., Pina, P., Vieira, G., Bandeira, L., Mora, C., 2018. Evaluation of the use of very high resolution aerial imagery for accurate ice-wedge polygon mapping (Adventdalen, Svalbard). *Sci. Total Environ.* 615, 1574–1583. <https://doi.org/10.1016/j.scitotenv.2017.09.153>.
- Lønne, I., 2005. Faint traces of high Arctic glaciations: an early Holocene ice-front fluctuation in Bolterdalen, Svalbard. *Boreas* 34, 308–323. <https://doi.org/10.1111/j.1502-3885.2005.tb01103.x>.
- Luffman, I., Nandi, A., 2019. Freeze-Thaw Induced Gully Erosion: A Long-Term High-Resolution Analysis. *Agronomy* 9, 549. <https://doi.org/10.3390/agronomy9090549>.
- Malamud, B.D., Turcotte, D.L., Guzzetti, F., Reichenbach, P., 2014. Landslide inventories and their statistical properties. *Earth Surf. Process. Land.* 29, 687–711. <https://doi.org/10.1002/esp.1064>.
- Martins, B., Meira-Castro, A., Nunes, A., Lourenço, L., 2020. The development of gullies in a Mediterranean environment: The example of the Corgo gully (central Portugal). *Energy Rep.* 6, 794–799. <https://doi.org/10.1016/j.egy.2019.11.004>.
- Mattsson, J., Flyen, A.-C., Nunez, M., 2010. Wood-decaying fungi in protected buildings and structures on Svalbard. *Agarica* 29, 5–14.
- Montanarella, L., Panagos, P., 2021. The relevance of sustainable soil management within the European Green Deal. *Land Use Policy* 100, 104950. <https://doi.org/10.1016/j.landusepol.2020.104950>.
- Nicu, I.C., 2018. Is Overgrazing Really Influencing Soil Erosion? *Water* 10, 1077. <https://doi.org/10.3390/w10081077>.
- Nicu, I.C., 2019. Natural risk assessment and mitigation of cultural heritage sites in North-eastern Romania (Valea Oii river basin). *Area* 51, 142–154. <https://doi.org/10.1111/area.12433>.
- Nicu, I.C., Stalsberg, K., Rubensdotter, L., Martens, V.V., Flyen, A.-C., 2020. Coastal Erosion Affecting Cultural Heritage in Svalbard. A Case Study in Hiorthhamn (Adventfjorden)—An Abandoned Mining Settlement. *Sustainability* 12, 2306. <https://doi.org/10.3390/su12062306>.
- Nicu, I.C., 2021. Is digital shoreline analysis system “fit” for gully erosion assessment? *CATENA* 203, 105307. <https://doi.org/10.1016/j.catena.2021.105307>.
- Nicu, I.C., Rubensdotter, L., Stalsberg, K., Nau, E., 2021a. Coastal Erosion of Arctic Cultural Heritage in Danger: A Case Study from Svalbard, Norway. *Water* 13, 784. <https://doi.org/10.3390/w13060784>.
- Nicu, I.C., Lombardo, L., Rubensdotter, L., 2021b. Preliminary Assessment of Thaw Slump Hazard to Arctic Cultural Heritage in Nordsenkiöld Land, Svalbard. *Landslides* 18, 2935–2947. <https://doi.org/10.1007/s10346-021-01684-8>.
- Nielsen, R.H., 2006. *Nature and Cultural Environments in the Arctic. Greenland, Iceland and Svalbard, TemaNord*, p. 45.
- Norwegian Polar Institute/USGS Landsat, 2021. Available online at <https://geodata.npolar.no>. (access 28 May 2021).
- Norwegian Polar Institute, 2021. <https://toposvalbard.npolar.no> (accessed 10 May 2021).
- Norwegian Polar Institute, 2021. <https://geokart.npolar.no/Html5Viewer/index.html?viewer=Svalbardkartet>. (accessed 10 September 2021).
- Oberle, F.K.J., Gibbs, A.E., et al., 2019. Towards determining spatial methane distribution on Arctic permafrost bluffs with an unmanned aerial system. *SN Appl. Sci.* 1, 236. <https://doi.org/10.1007/s42452-019-0242-9>.
- Obu, J., Westermann, S., Bartsch, A., et al., 2019. Northern Hemisphere permafrost map based on TTOP modelling for 2000–2016 at 1 km² scale. *Earth Sci. Rev.* 193, 299–316. <https://doi.org/10.1016/j.earscirev.2019.04.023>.
- Pastor, A., Poblador, S., Skovsholt, L.J., Riis, T. Microbial carbon and nitrogen processes in high-Arctic riparian soils. *Permafrost and Periglac. Process.* 31, 223–236. doi: 10.1002/ppp.2039.
- Perreault, N., Lévesque, E., Fortier, D., Lamarque, L.J., 2016. Thermo-erosion gullies boost the transition from wet to mesic tundra vegetation. *Biogeosciences* 13, 1237–1253. <https://doi.org/10.5194/bg-13-1237-2016>.
- Perreault, N., Lévesque, E., Fortier, D., Gratton, D., Lamarque, L.J., 2017. Remote sensing evaluation of High Arctic wetland depletion following permafrost disturbance by thermo-erosion gully processes. *Arctic Science* 3, 237–253. <https://doi.org/10.1139/as-2016-0047>.
- Prestvold, K., 2008. Svalbard's cultural remains – traces of history in an Arctic landscape. Norwegian Polar Institute, *Cruise Handbook for Svalbard* <http://cruise-handbook.npolar.no/en/svalbard/cultural-remains.html> (accessed on 15 September 2021).
- Romashova, K.V., Chernov, R.A., Vasilevich, I.I., 2019. Study of the glacial flow of rivers in the Gronfjord bay basin (Western Svalbard). *Arctic and Antarctic Research* 65, 34–45. <https://doi.org/10.30758/0555-2648-2019-65-1-34-45>.
- Saha, A., et al., 2021. Modelling multi-hazard threats to cultural heritage sites and environmental sustainability: The present and future scenarios. *J. Clean. Prod.* 320, 128713. <https://doi.org/10.1016/j.jclepro.2021.128713>.
- Schuur, E.A.G., et al., 2015. Climate change and the permafrost carbon feedback. *Nature* 520, 171–179. <https://doi.org/10.1038/nature14338>.
- Sesana, E., Gagnon, A.S., Ciantelli, C., Cassar, J., Hughes, J.J., 2021. Climate change impacts on cultural heritage: A literature review. *Wires Clim. Change* 12, e710. <https://doi.org/10.1002/wcc.710>.
- Sidle, R.C., Jarihani, B., et al., 2019. Hydrogeomorphic processes affecting dryland gully erosion: Implications for modelling. *Prog. Phys. Geogr.* 43, 46–64. <https://doi.org/10.1177/0309133318819403>.
- Sidorchuk, A., 1999. Dynamic and static models of gully erosion. *CATENA* 37, 401–414. [https://doi.org/10.1016/S0341-8162\(99\)00029-6](https://doi.org/10.1016/S0341-8162(99)00029-6).
- Sidorchuk, A., 2006. Stages in gully evolution and self-organized criticality. *Earth Surf. Proc. Land.* 31, 1329–1344. <https://doi.org/10.1002/esp.1334>.
- Sidorchuk, A., 2020. The Potential of Gully Erosion on the Yamal Peninsula, West Siberia. *Sustainability* 12, 260. <https://doi.org/10.3390/su12010260>.
- Sidorchuk, A., Matveeva, T.A., 2020. Periglacial gully erosion on the East European Plain and its recent analog at the Yamal Peninsula. *Geography, Environment, Sustainability* 13, 183–194. <https://doi.org/10.24057/2071-9388-2019-01>.

- Stange, R., 2019. The old airfield. https://www.spitsbergen-svalbard.com/photos-panoramas-videos-and-webcams/spitsbergen-panoramas/old-airfield.html#Adventdalen_19Juni13_06 (accessed 15 September 2021).
- Strozzi, T., Paul, F., Wiesmann, A., Schellenberger, T., Kääb, A., 2017. Circum-Arctic Changes in the Flow of Glaciers and Ice Caps from Satellite SAR Data between the 1990s and 2017. *Remote Sens.* 9, 947. <https://doi.org/10.3390/rs9090947>.
- Tanyas, H., Allstadt, K.E., van Westen, C.J., 2018. An updated method for estimating landslide-event magnitude. *Earth Surf. Proc. Land.* 43, 1836–1847. <https://doi.org/10.1002/esp.4359>.
- Tape, K.D., Verbyla, D., Welker, J.M., 2011. Twentieth century erosion in Arctic Alaska foothills: The influence of shrubs, runoff, and permafrost. *J. Geophys. Res.* 116, G04024. <https://doi.org/10.1029/2011JG001795>.
- ten Brink, U.S., Barkan, R., Andrews, B.D., Chaytor, J.D., 2009. Size distributions and failure initiation of submarine and subaerial landslides. *Earth Planet. Sc. Lett.* 287, 31–42. <https://doi.org/10.1016/j.epsl.2009.07.031>.
- Thuestad, A.E., Tømmervik, H., Solbø, S.A., 2015. Assessing the impact of human activity on cultural heritage in Svalbard: a remote sensing study of London. *The Polar Journal* 5, 428–445. <https://doi.org/10.1080/2154896X.2015.1068536>.
- van Pelt, W., Pohjola, V., et al., 2019. A long-term dataset of climatic mass balance, snow conditions, and runoff in Svalbard (1957–2018). *The Cryosphere* 13, 2259–2280. <https://doi.org/10.5194/tc-13-2259-2019>.
- Vanmaercke, M., Panagos, P., et al., 2021. Measuring, modelling and managing gully erosion at large scales: A state of the art *Earth-Sci. Rev.* 103637 <https://doi.org/10.1016/j.earscirev.2021.103637>.
- Zagórski, P., Jarosz, K., Superson, J., 2020. Integrated assessment of shoreline change along the Calypsostranda (Svalbard) from remote sensing, field survey and GIS. *Mar. Geod.* 43, 433–471. <https://doi.org/10.1080/01490419.2020.1715516>.
- Zwoliński, Z. et al., 2013. Geomorphological settings of Polish research areas on Spitsbergen. *Landform Analysis* 22, 125–143. <http://doi.org/10.12657/landfana.022.011>.